PCCP

ROYAL SOCIETY OF CHEMISTRY

PAPER

View Article Online
View Journal | View Issue

Cite this: *Phys. Chem. Chem. Phys.*, 2024, **26**, 23703

Rotational spectra of five cyano derivatives of fluorene†

Carlos Cabezas, *[a] Jesús Janeiro, [b] Amanda L. Steber, [c] Dolores Pérez, [b] Celina Bermúdez, [c] Enrique Guitián, [b] Alberto Lesarri [c] and José Cernicharo[a]

Received 8th May 2024,
Accepted 19th August 2024

DOI: 10.1039/d4cp01924e

rsc.li/pccp

The recent interstellar detection of individual polycyclic aromatic hydrocarbons (PAHs) in the dense molecular cloud TMC-1 brings interest in related species that could be present in this astronomical environment. These detections, that include pure PAHs and their cyano-derivative counterparts, were performed through the interplay between laboratory rotational spectroscopy experiments and radioastronomical observations. Here, we present the laboratory rotational spectroscopic study of the five cyano-derivatives of the PAH fluorene ($C_{13}H_{10}$). The samples for these five species were synthetized in the laboratory and then characterized in the gas phase using a chirped-pulse Fourier-transform microwave spectrometer operating between 2 and 12 GHz. The analysis of the rotational spectra allowed us to derive accurate molecular constants for the five isomers used to obtain frequency predictions that enable astronomical searches of these molecules in the interstellar medium.

Introduction

Polycyclic aromatic hydrocarbons (PAHs) are considered the most abundant family of molecules in the universe based on the strength and ubiquity of the unidentified infrared (UIR) bands. In fact, in the interstellar medium (ISM), 10%–25% of all carbon may be locked in large PAHs.[1] Despite their apparent omnipresence, there are several aspects about interstellar PAHs that are not yet well understood, *e.g.* their formation and evolution remain poorly constrained. Two contradictory pathways have been proposed for PAH production: the "top-down" and the "bottom-up" scenarios. The first one suggests that multiringed species like fullerenes are formed in the hot and dense outflows of carbon-rich evolved stars.[1–3] Subsequent processing of these species in diffuse clouds generates smaller species in high abundances. In the "bottom-up" scenario, complex molecules are built up from small carbon chains in the cold and shielded environments of dark clouds. Knowledge on the abundance of individual PAHs in combination with astrochemical modeling will shed light on this problem, so that we may be able to differentiate between the two formation pathways. However, information about individual PAHs has remained unavailable for decades due to the inability to detect any specific PAH.

The interplay of laboratory spectroscopy and radio astronomy provides the most powerful means of identifying molecular species in the ISM. Rotational transitions for molecular species can be measured with remarkably high precision ($>10^6:1$) across an extremely wide frequency range (cm- to sub-mm wave). As a consequence, the rotational transitions detected by radio astronomy represent a unique molecular fingerprint and the basis for an unambiguous identification. The discovery of about 90% of the more than 320 molecules detected in space has been achieved *via* their rotational emission using radio astronomy.[4–6] However, PAHs are often highly symmetric and therefore possess no permanent electric dipole moment or, when they are not symmetric, they are weakly polar at best, making PAHs notoriously difficult, if not impossible, to detect by this approach. In fact, the first observation of a pure (*i.e.*, containing only carbon and hydrogen) PAH, indene (C_9H_8), in the ISM was achieved very recently, thanks to the high level of sensitivity of the line surveys QUIJOTE[7] (Q-band Ultrasensitive Inspection Journey to the Obscure TMC-1 Environment) and GOTHAM[8] (GBT Observations of TMC-1: Hunting for Aromatic Molecules) obtained with the Yebes 40m telescope and the Green Bank Telescope. In 2021, indene was discovered in the cold pre-stellar core Taurus molecular cloud (TMC-1).[9,10] Indene is composed of a six- and a five-membered ring with a small but appreciable (~0.6 D) dipole moment.[11] Its relatively high abundance in TMC-1[9,10] helped

[a] *Departamento de Astrofísica Molecular, Instituto de Física Fundamental (IFF–CSIC), C/Serrano 121, Madrid 28006, Spain. E-mail: carlos.cabezas@csic.es*
[b] *Centro Singular de Investigación en Química Biolóxica e Materiais Moleculares (CiQUS) and Departamento de Química Orgánica, Universidade de Santiago de Compostela, Santiago de Compostela 15782, Spain*
[c] *Departamento de Química Física y Química Inorgánica, Facultad de Ciencias-I.U. CINQUIMA, Universidad de Valladolid, Valladolid E-47011, Spain*

† Electronic supplementary information (ESI) available: Synthesis and characterization data, linelists, molecular parameters and fit result files of the five CNF species. See DOI: https://doi.org/10.1039/d4cp01924e

the observation and identification of its rotational transitions in the ISM. Besides indene, the cyano-derivatives of some PAHs, like indene itself (C_9H_7CN) and naphthalene ($C_{10}H_7CN$), were also found in TMC-1,[12,13] together with other cyano- and ethynyl-derivatives of organic rings[9,14–18] like cyclopropenylidene, cyclopentadiene and benzene.

Replacing even a single hydrogen on a pure PAH with a polar functional group, such as the nitrile (or cyano) unit, –C≡N, yields a surrogate with a largely increased dipole moment with respect to the PAH counterpart, making it much easier to detect. In the case of indene, for example, the dipole moment when passing from C_9H_8 to C_9H_7CN increases from 0.6 to 4.75 D.[13] It is true that the cyano-derivatives are less abundant than the unsubstituted counterparts, as estimates based on the observed abundances in TMC-1 indicate a quotient C_9H_8/C_9H_7CN = ∼20–40.[13] However, the lower abundance of this species is compensated, in terms of the intensity of the rotational transitions, thanks to the much larger value of the dipole moment, in the case of C_9H_7CN by a factor of ∼63. In addition, it has been suggested that the cyano-derivatives of PAHs can be used as an excellent observational proxy for their hydrocarbon counterparts for constraining models. All these points render the strategy of searching for cyano derivatives of PAHs extremely tantalizing.

In this paper, we present the pure rotational spectra of the five monocyano-derivatives (Fig. 1) of the PAH fluorene ($C_{13}H_{10}$), also known as 9*H*-fluorene. The molecule of fluorene has a total of five non-equivalent hydrogen atoms which might be substituted by a cyano group. While the parent fluorene has been characterized by rotational spectroscopy, in spite of its weak dipole moment, ∼0.53 D,[19] to the best of our knowledge, there is not any spectroscopy information available in the literature on its cyano-derivatives. To carry out the spectroscopic study of the five isomers of cyanofluorene (CNF hereafter), we have synthesized the samples in the laboratory. Rotational spectroscopy measurements were performed using high resolution chirped-pulse Fourier transform microwave spectroscopy in the 2–12 GHz frequency region. From these measurements, we derived precise spectroscopic constants that will be the basis for further astronomical searches of these molecular species in the ISM.

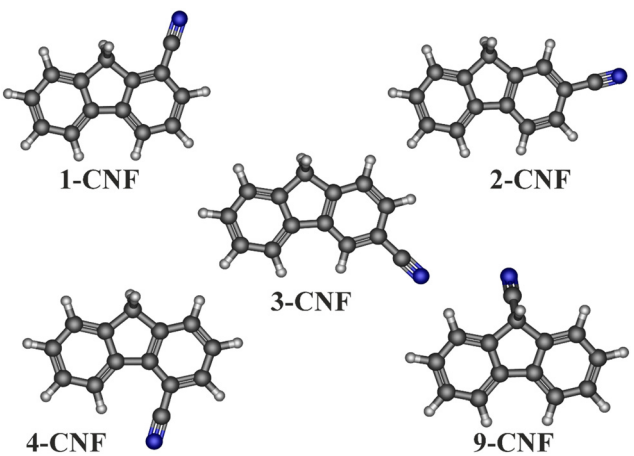

Fig. 1 Molecular structures of the five CNF isomers.

Experimental methods

Synthesis

All reactions were carried out under argon using oven-dried glassware. Anhydrous DMSO, CH_2Cl_2, Et_2O, toluene and DMF were obtained from an MBraun SPS-800 Solvent Purification System. Commercial reagents were purchased from ABCR GmbH, Sigma-Aldrich or Fluorochem, and were used without further purification. TLC was performed on Merck silica gel 60 F_{254} and chromatograms were visualized with UV light (254 and 360 nm). Column chromatography was performed on Merck silica gel 60 (ASTM 230–400 mesh). Centrifugation was performed in a Hettich EBA21 centrifuge. ^{1}H and ^{13}C NMR spectra were recorded at 300 and 75 MHz (Varian Mercury-300 instrument), 400 and 101 MHz (Varian Inova 400) or 500 and 125 MHz (Varian Inova 500), respectively. Low resolution mass spectra (EI) were obtained at 70 eV on an HP-5988A instrument, while high-resolution mass spectra (HRMS) were obtained on a Micromass AutoSpec spectrometer. Atmospheric pressure chemical ionisation (APCI) HRMS spectra were obtained on a Bruker micrOTOF using either a direct inlet probe (DIP) or flow injection analysis (FIA) for sample introduction. See the ESI† for the experimental details and characterization data.

Quantum chemical calculations

Prior to the spectroscopic experiments, we performed quantum chemical calculations to obtain the molecular parameters of CNF species necessary to interpret the rotational spectra. Geometry optimizations for all five isomers were performed using the density functional theory (DFT) variant B3LYP[20] and the correlation-consistent polarized valence basis set cc-pVTZ.[21] We chose this calculation method since it was employed by Thorwirth *et al.*[19] to predict the rotational constants of fluorene with reasonable results. The values for the rotational constants,

Table 1 Molecular constants and relative energies for the five CNF isomers calculated at the B3LYP/cc-pVTZ level of theory

	1-CNF	2-CNF	3-CNF	4-CNF	9-CNF
A/MHz	1318.2	2158.5	1553.1	1037.8	967.7
B/MHz	438.6	331.6	372.4	557.2	571.1
C/MHz	329.8	288.0	300.9	363.3	373.1
Δ_J/kHz	0.0048	0.0012	0.0025	0.0180	0.0394
Δ_{JK}/kHz	−0.0194	0.0032	0.0049	0.0038	−0.0457
Δ_K/kHz	0.1063	0.0965	0.1338	−0.0200	0.0103
δ_J/kHz	0.0016	−0.0002	0.0007	0.0055	0.0154
δ_K/kHz	0.0126	−0.0077	0.0164	0.0244	0.0101
χ_{aa}/MHz	0.076	−4.527	−2.582	2.507	2.442
χ_{bb}/MHz	−2.228	2.458	0.475	−4.623	−2.753
$\lvert\mu_a\rvert$/D	3.2	5.4	4.8	0.4	0.0
$\lvert\mu_b\rvert$/D	2.9	0.1	2.9	4.8	3.6
$\lvert\mu_c\rvert$/D	0.0	0.0	0.0	0.0	1.9
ΔE^a/cm^{-1}	65	0	145	180	2138

[a] Relative energy to that of the 2-CNF isomer.

^{14}N nuclear quadrupole coupling constants, and electric dipole moment components were derived from these calculations. In addition, harmonic vibrational frequencies were computed at the same level of theory to estimate the values of the centrifugal distortion constants. The results from the quantum chemical calculations, including the relative energies, are shown in Table 1, while the optimized molecular structures for the five CNF isomers are displayed in Fig. 1. All the calculations were performed using the Gaussian 16 program package.[22]

Rotational spectroscopy experiments

The experimental setup employed in this work consists of a broadband chirped-pulse Fourier transform microwave (CP-FTMW) spectrometer[23–25] at the Universidad de Valladolid and working over 2–12 GHz. The solid sample containing the five isomers was vaporized at ~130 °C in a solenoid-driven pulsed injector and diluted with an inert carrier gas (He/Ar mixture at 3 bar). The CNF species were expanded into an evacuated chamber generating molecular jet pulses (typ. 800 μs). The data were collected in a series of three measurements. In the first one, the molecules of each gas pulse were polarized with a series of 8 microwave pulses with a duration of 4 μs spanning 2–8 GHz. The measurement was performed at a repetition rate of 5 Hz, giving an effective repetition rate of 40 Hz. The 8–12 GHz regime was divided into two separate measurements, 2 GHz each, in which each gas pulse was probed with 5 microwave pulses. The operating repetition rate of the instrument was 1 Hz, giving an effective repetition rate of 5 Hz. The chirp pulses were generated with an arbitrary waveform generator (Tektronix AWG 70002A), amplified by 300 W with a traveling wave tube (TWT) amplifier in the case of the 2–8 GHz measurement and by 20 W with a solid-state MW amplifier in the case of the higher frequency measurements, and broadcast perpendicular to the propagation of the jet expansion through a horn antenna.

A molecular transient emission, of 40 μs in the case of 2–8 GHz and 20 μs in the case of the 8–12 GHz measurements, was then detected through a second horn and amplified by a low noise MW amplifier. A total of 700k FIDs from 2 to 8 GHz and 200k FIDs per measurement between 8 and 12 GHz were co-added on a digital oscilloscope (25 GS per s and 50 GS per s, respectively) and a Fourier transformation finally yielded the resonance frequencies of the rotational transitions. The use of a Kaiser–Bessel apodization window resulted in linewidths of *ca.* 100 kHz. The accuracy of the frequency measurements is better than 25 kHz. All frequency components are referenced to a Rb standard.

Results and discussion

The synthesis of the targeted CNFs was accomplished through different strategies depending on each particular isomer. Thus, 1-CNF was prepared by a nickel-catalyzed decarbonylative cyanation of fluorene-1-carbonyl chloride,[26] and 2-CNF and 4-CNF were obtained by cyano-debromination of the corresponding commercially available bromofluorenes, while, in contrast, 3-CNF was synthesized by palladium-catalyzed C–H bond activation and subsequent intramolecular arylation of 2′-bromo-3-cyano-6-methyl-1,1′-biphenyl.[27] Finally, the synthesis of 9-CNF was performed in three steps from the parent fluorene by the formation of 9-carbaldehyde, transformation in the corresponding oxime, and further dehydration.[28] The detailed experimental procedures are described in the ESI.†

As can be seen from Table 1, the five CNF isomers show at least one large electric dipole moment component which allows for a straightforward detection through their rotational spectra. Isomers 1-CNF, 2-CNF, 3-CNF and 4-CNF have a planar heavy-atom skeleton, with only the methylene group hydrogen atoms as the sole out-of-plane mass contributors. This manifests in the negative inertial defect values around 3.5 amu Å^2 (Table 2), typical for methylene groups. This fact causes the absence

Table 2 Experimental molecular parameters for the CNF isomers obtained in this work

	1-CNF	2-CNF	3-CNF	4-CNF	9-CNF
A/MHz	1303.70307(92)[a]	2140.700(87)	1541.8327(10)	1031.74077(27)	968.61817(48)
B/MHz	438.89904(23)	330.62387(37)	371.40436(23)	557.09884(28)	568.80591(40)
C/MHz	329.09001(14)	286.97931(34)	299.92528(17)	362.66718(23)	373.01098(40)
Δ_J/kHz	—	—	—	0.0206(18)	0.0359(14)
Δ_K/kHz	—	—	—	−0.0232(21)	—
χ_{aa}/MHz	0.213(72)	—	−2.280(39)	2.218(14)	2.235(45)
χ_{bb}/MHz	−2.111(21)	—	0.379(24)	−4.129(11)	−2.338(20)
Δ^b/amu Å^2	−3.418	−3.595	−3.496	−3.469	−55.191
N^c	55	28	40	89	62
$N_{hfc}{}^d$	155	—	108	265	181
J_{max}	11	13	12	16	15
$K_{a\,max}$	4	4	4	6	5
μ_a	Observed	Observed	Observed	Not observed	Not observed
μ_b	Observed	Not observed	Observed	Observed	Observed
μ_c	Not observed	Not observed	Not observed	Not observed	Observed
σ^e/kHz	11.9	10.0	12.8	15.1	17.6

[a] Values in parentheses denote 1σ errors, applied to the last digit. [b] Inertial defect, $\Delta = I_c - I_b - I_a$. [c] Number of rotational transitions included in the fit. [d] Number of hyperfine components included in the fit. [e] rms error of the fit.

Table 3 Experimental and theoretical molecular parameters for the fluorene molecule

	Experimental[a]	B3LYP/cc-pVTZ[b]
A/MHz	2176.210153(70)	2195.0
B/MHz	586.653414(70)	588.2
C/MHz	463.569028(20)	465.2
Δ_J/kHz	0.00473(18)	0.00423
Δ_{JK}/kHz	−0.00468(84)	−0.00308
Δ_K/kHz	0.0984(11)	0.0948
δ_J/kHz	0.001243(88)	0.00103
δ_K/kHz	0.0175(31)	0.0123

[a] Thorwirth *et al.*[19] [b] This work.

of *c*-type rotational transitions for any of the four species because the electric dipole moment component along the *c* axis must be zero for a planar skeleton. In contrast, the isomer 9-CNF shows a much more pronounced negative inertial defect value due to the substitution of one of the methylene hydrogen atoms by the cyano group; see Fig. 1. This induces a strong electric dipole moment component along the *c* axis and the lack, in this case, of a μ_a dipole moment component.

Table 3 shows the results that we obtained for the rotational and centrifugal distortion constants of fluorene at the B3LYP/cc-pVTZ level of calculation, as well as the experimental values for these constants determined by Thorwirth *et al.*[19] To facilitate the assignment process of the rotational transitions of the CNF isomers, the theoretical values for the rotational constants of each CNF isomer were scaled using the experimental/theoretical ratio obtained from the fluorene molecule. Using these corrected constants, we identified the five CNF isomers in our broadband spectrum. Fitting of experimental data was done with the SPFIT program[29] utilizing Watson's *A*-reduced asymmetric rotor Hamiltonian in the I^r (isomers 1-, 2-, 3- and 9-CNF) and III^l (isomer 4-CNF) representation.[30] The presence of a ^{14}N-nitrogen nucleus, which has a nonzero nuclear spin (I = 1), in the CNF isomers causes each rotational transition to be split into several hyperfine components because of the nuclear quadrupole coupling effects; see Fig. 2. This effect, due to the interaction at the nitrogen nucleus of the quadrupole moment with the electric field gradient created by the rest of the molecular charges, causes the coupling of the nuclear spin moment to the overall rotational momentum.[31] To account for such hyperfine effects, the employed rotational Hamiltonian has the following form: $H = H_R + H_Q$, where H_R contains rotational and centrifugal distortion parameters, while H_Q describes the quadrupole coupling terms. The coupling scheme is $\mathbf{F} = \mathbf{J} + \mathbf{I}$ (N), where I (N) = 1. The energy levels involved in each transition are labelled with the quantum numbers J, K_a, K_c and F.

The most stable CNF isomer is 2-CNF. For this species, we observed a total of 28 rotational transitions, all of them being *a*-type ones since the dipole moment components along the *a* and *b* axes are 5.4 and 0.1 D, respectively. In spite of the fact that all rotational transitions for CNF isomers are split, the hyperfine structure for the *a*-type transitions of 2-CNF could not be resolved at the spectral resolution of our broadband spectrometer. For this reason, we could only determine the rotational constants A, B and C for the 2-CNF isomer (Table 2), which were obtained from a fit where the centrifugal distortion constant values were kept fixed to those derived from quantum chemical calculations. The isomers 1-CNF and 3-CNF are the two next stable species and both have appreciable *a*- and *b*-type dipole moment components. The observed rotational transitions for 1-CNF and 3-CNF isomers encompass a total of 155 and 108 hyperfine components which, unlike the case of the isomer 2-CNF, were well resolved in both *a*- and *b*-type transitions. In this manner, the rotational constants as well as the nuclear quadrupole coupling constants, χ_{aa} and χ_{bb}, could be derived from the fits for 1-CNF and 3-CNF isomers. The values are shown in Table 2. In the case of the 4-CNF isomer, however, there is a very large dipole moment component along the *b* axis and a tiny μ_a component. Its rotational transitions are the most intense ones and dominate the spectrum shown in Fig. 2. A total of 265 hyperfine components from 89 *b*-type rotational transitions were measured for the 4-CNF isomer (see an example in Fig. 2) and fitted, using the III^l representation, to obtain the rotational, the Δ_J and Δ_K quartic centrifugal distortion constants and nuclear quadrupole coupling constants, which are shown in Table 2. Finally for the 9-CNF isomer, the least stable isomer, we were able to detect a total of 181 hyperfine components including *b*- and *c*-type ones. The experimentally derived constants for the 9-CNF isomer include not

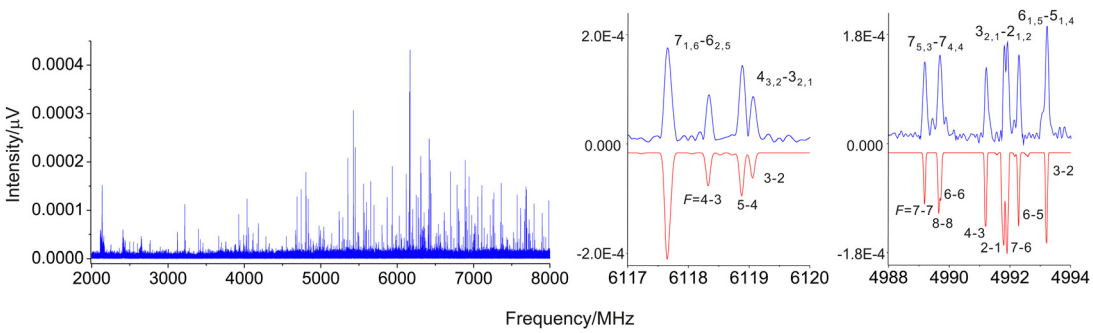

Fig. 2 Displayed in the left panel is the 700k average broadband rotational spectrum of the five CNF isomers from 2 to 8 GHz. The insets display several rotational transitions of 9-CNF (middle) and 4-CNF (right) showing the nuclear quadrupole hyperfine structure. The blue trace is the experimental spectrum and the red one is the simulated (at 2.5 K) spectrum based on the fitted molecular constants for each isomer.

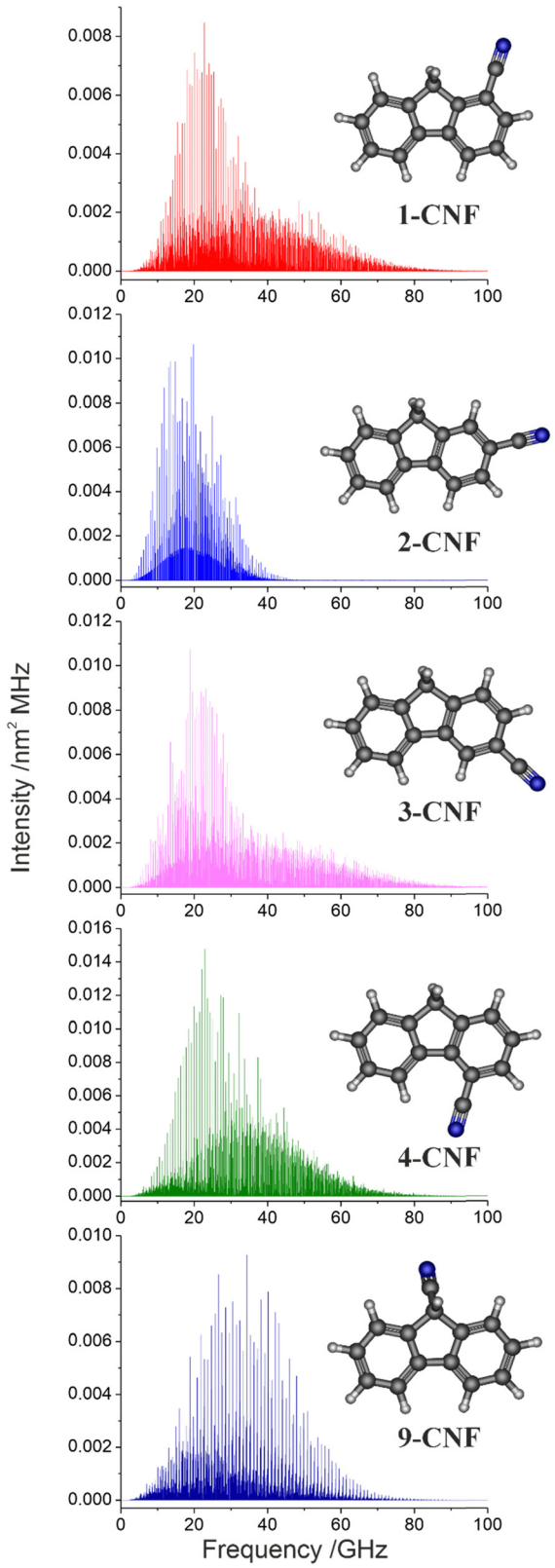

Fig. 3 The simulated spectra of the five CNF isomers at 9 K.

only the rotational and diagonal nuclear quadrupole coupling constants, but also the quartic centrifugal distortion constant Δ_J.

Table 4 Rotational partition functions for the five CNF isomers at different temperatures

Temperature/K	1-CNF	2-CNF	3-CNF	4-CNF	9-CNF
300.00	1808258.8	1655769.1	1835089.3	1770180.7	1788845.9
225.00	1249796.5	1165895.1	1284122.6	1207915.8	1219049.0
150.00	706952.7	673180.9	735694.9	675241.8	680468.2
75.00	252361.6	242893.8	264210.9	239945.4	241659.9
37.50	89232.3	85913.0	93433.8	84823.9	85429.6
18.75	31551.7	30378.1	33036.7	29991.0	30205.3
9.00	10495.7	10104.9	10989.2	9976.4	10047.7

The list of measured lines and the results from the fits for the five isomers are given in the ESI.†

The experimental (ground-state) rotational constants obtained in this work for the CNF isomers are in good agreement with those (equilibrium) derived from our DFT calculations at the B3LYP/cc-pVTZ level of theory. The relative errors range from 0.02 to 0.4% for the *B* and *C* rotational constants, while they are larger, between 0.2 and 1.1%, for the *A* constants. In the same manner, the experimental values for the nuclear quadrupole coupling constants, χ_{aa} and χ_{bb}, are in accordance with those obtained theoretically, as can be seen from Tables 1 and 2. Regarding the centrifugal distortion constants, those determined for 4-CNF and 9-CNF isomers are in agreement with the values obtained from our calculations.

The data from Table 3 indicate that the B3LYP/cc-pVTZ level of theory provides reasonable values for the quartic centrifugal distortion constants for fluorene, probably due to its molecular rigidity. Hence, a similar level of accuracy can be expected for the predicted values of the centrifugal constants of other rigid molecules like the CNF isomers. For this reason, as mentioned above, in the fitting procedure for the five isomers we included the values for the five quartic centrifugal distortion constants, which were kept fixed to the values obtained from our DFT calculations. This approach was found to have little impact on the fitted values of the rotational constants that change only within their uncertainties when distortion constants are not included. However, it should enable a more reliable extrapolation of transition frequencies into higher frequency regions, where the astronomical searches will be done.

The most promising astronomical source where the CNF isomers could be detected is the cold dark cloud TMC-1, given that other large organic rings have been detected there recently. Assuming a rotational temperature of 9 K, which is the gas kinetic temperature in TMC-1,[32] the most intense rotational transitions for the CNF isomers are expected to be in the microwave K-band, between 18 and 27 GHz, as can be seen from Fig. 3. The frequency predictions for the five isomers were derived from the rotational constants from Table 2, using the SPCAT program,[29] which was also employed to calculate the partition functions, at a maximum value of $J = 200$ and without hyperfine constants, shown in Table 4. Even though the frequency range of our laboratory observations is not very wide, the frequency extrapolation of our predictions may be feasible, up to 27 GHz, due to the accuracy of the obtained molecular constants and to the particular rigidity shown by these

molecules, which causes several *K*-components of a given *J* rotational level to collapse to a single line. Transition frequencies over this frequency range should be viewed with caution, even those with K_a values of 0 and 1. This, combined with fairly large dipole moment components, leads to a comparably strong rotational spectrum and makes CNF isomers plausible targets for astronomical searches in the K-band frequency region.

Conclusions

In this work, we have investigated the pure rotational spectra for the five monocyano derivatives of fluorene. The chemical samples for these species were synthetized in the laboratory and probed in the gas phase by broadband Fourier-transform microwave spectroscopy in the 2–12 GHz frequency region. From the analysis of the rotational spectra, we obtained accurate rotational and ^{14}N nuclear quadrupole coupling parameters for the five isomers. These sets of molecular constants will allow us to obtain frequency predictions for the five species that can be used as a guide for further astrophysical searches in cold molecular clouds like TMC-1.

Author contributions

Carlos Cabezas: conceptualization, data curation, formal analysis, project administration, writing – original draft. Jesús Janeiro: synthesis and characterization, writing – review and editing. Amanda L. Steber: data acquisition and analysis, writing – review and editing. Dolores Pérez: conceptualization, supervision and funding acquisition for the synthetic work, writing – original draft. Celina Bermúdez: data acquisition, writing – review and editing. Enrique Guitián: synthesis and characterization, writing – review and editing. Alberto Lesarri: funding acquisition, writing – review and editing. José Cernicharo: funding acquisition, writing – review and editing.

Data availability

The data supporting this article have been included as part of the ESI.†

Conflicts of interest

There are no conflicts to declare.

Acknowledgements

CC and JC thank the Ministerio de Ciencia e Innovación of Spain (MICIU) for funding support through project PID2019-107115GB-C21/AEI/10.13039/501100011033, the Consejo Superior de Investigaciones Científicas (CSIC; Spain) for funding through project PIE 202250I097, and also thank ERC for funding through grant ERC-2013-Syg-610256-NANOCOSMOS. DP and EG acknowledge the financial support from grant PID2022-139933NB-I00, funded by MCIN/AEI/10.13039/501100011033, the Xunta de Galicia (Centro singular de investigación de Galicia accreditation 2019–2022, ED431G 2019/03) and the European Union (European Regional Development Fund – ERDF). JJ thanks the Agencia Estatal de Investigación for the award of pre-doctoral fellowship PRE2020-092897. ALS, CB and AL thank the Ministerio de Ciencia e Innovación of Spain (MICIU) for funding support through projects PID2022-139933NB-I00 and PID2022-136525NA-I00, the Junta de Castilla y León and the European Regional Development Funds (ERDF) for funding under project INFRARED IR2021-UVa13. ALS acknowledges that this project has received funding from the European Union Horizon 2020 research and innovation program under the Marie Skłodowska Curie grant agreement no. 894433 – AstroSsearch. CB thanks Ministerio de Universidades for a ''Maria Zambrano'' grant at UVa (CONVREC-2021-317).

References

1 A. G. G. M. Tielens, Interstellar polycyclic aromatic hydrocarbon molecules, *Annu. Rev. Astron. Astrophys.*, 2008, **46**, 289–337.
2 S. Kwok and Y. Zhang, Mixed aromatic–aliphatic organic nanoparticles as carriers of unidentified infrared emission features, *Nature*, 2011, **479**, 80–83.
3 L. Martínez, G. Santoro, P. Merino, M. Accolla, K. Lauwaet, J. Sobrado, H. Sabbah, R. J. Pelaez, V. J. Herrero, I. Tanarro, M. Agúndez, A. Martín-Jimenez, R. Otero, G. J. Ellis, C. Joblin, J. Cernicharo and J. A. Martín-Gago, Prevalence of non-aromatic carbonaceous molecules in the inner regions of circumstellar envelopes, *Nat. Astron.*, 2019, **4**, 97–105.
4 B. A. McGuire, 2021 Census of Interstellar, Circumstellar, Extragalactic, Protoplanetary Disk, and Exoplanetary Molecules, *Astrophys. J., Suppl. Ser.*, 2022, **259**, 30.
5 H. S. P. Müller, The Cologne Database for Molecular Spectroscopy (CDMS), **https://cdms.astro.uni-koeln.de/classic/molecules**.
6 D. E. Woon, The Astrochymist, **https://www.astrochymist.org/**.
7 J. Cernicharo, M. Agúndez, R. I. Kaiser, C. Cabezas, B. Tercero, N. Marcelino, J. R. Pardo and P. de Vicente, Discovery of benzyne, o-C_6H_4, in TMC-1 with the QUIJOTE line survey, *Astron. Astrophys.*, 2021, **652**, L9.
8 B. A. McGuire, A. M. Burkhardt, S. Kalenskii, C. N. Shingledecker, A. J. Remijan, E. Herbst and M. C. McCarthy, Detection of the aromatic molecule benzonitrile (c-C_6H_5CN) in the interstellar medium, *Science*, 2018, **359**, 202–205.
9 J. Cernicharo, M. Agúndez, C. Cabezas, B. Tercero, N. Marcelino, J. R. Pardo and P. de Vicente, Pure hydrocarbon cycles in TMC-1: Discovery of ethynyl cyclopropenylidene, cyclopentadiene, and indene, *Astron. Astrophys.*, 2021, **649**, L15.
10 A. M. Burkhardt, K. Long Kelvin Lee, P. Bryan Changala, C. N. Shingledecker, I. R. Cooke, R. A. Loomis, H. Wei, S. B. Charnley, E. Herbst, M. C. McCarthy and B. A. McGuire,

Discovery of the Pure Polycyclic Aromatic Hydrocarbon Indene (c-C_9H_8) with GOTHAM Observations of TMC-1, *Astrophys. J., Lett.*, 2021, **913**, L18.

11 W. Caminati, Low-energy vibrations of indene, *J. Chem. Soc., Faraday Trans.*, 1993, **89**, 4153.

12 B. A. McGuire, R. A. Loomis, A. M. Burkhardt, K. L. K. Lee, C. N. Shingledecker, S. B. Charnley, I. R. Cooke, M. A. Cordiner, E. Herbst, S. Kalenskii, M. A. Siebert, E. R. Willis, C. Xue, A. J. Remijan and M. C. McCarthy, Detection of two interstellar polycyclic aromatic hydrocarbons via spectral matched filtering, *Science*, 2021, **371**, 1265–1269.

13 M. L. Sita, P. B. Changala, C. Xue, A. M. Burkhardt, C. N. Shingledecker, K. L. Kelvin Lee, R. A. Loomis, E. Momjian, M. A. Siebert, D. Gupta, E. Herbst, A. J. Remijan, M. C. McCarthy, I. R. Cooke and B. A. McGuire, Discovery of Interstellar 2-Cyanoindene (2-C_9H_7CN) in GOTHAM Observations of TMC-1, *Astrophys. J., Lett.*, 2022, **938**, L12.

14 M. C. McCarthy, K. L. K. Lee, R. A. Loomis, A. M. Burkhardt, C. N. Shingledecker, S. B. Charnley, M. A. Cordiner, E. Herbst, S. Kalenskii, E. R. Willis, C. Xue, A. J. Remijan and B. A. McGuire, Interstellar detection of the highly polar five-membered ring cyanocyclopentadiene, *Nat. Astron.*, 2020, **5**, 176–180.

15 K. L. Kelvin Lee, P. B. Changala, R. A. Loomis, A. M. Burkhardt, C. Xue, M. A. Cordiner, S. B. Charnley, M. C. McCarthy and B. A. McGuire, Interstellar Detection of 2-cyanocyclopentadiene, C_5H_5CN, a Second Five-membered Ring toward TMC-1, *Astrophys. J. Lett.*, 2021, **910**, L2.

16 J. Cernicharo, M. Agúndez, R. I. Kaiser, C. Cabezas, B. Tercero, N. Marcelino, J. R. Pardo and P. de Vicente, Discovery of two isomers of ethynyl cyclopentadiene in TMC-1: Abundances of CCH and CN derivatives of hydrocarbon cycles, *Astron. Astrophys.*, 2021, **655**, L1.

17 C. Cabezas, M. Agúndez, R. Fuentetaja, Y. Endo, N. Marcelino, B. Tercero, J. R. Pardo, P. de Vicente and J. Cernicharo, Discovery of the cyclic C_5H radical in TMC-1, *Astron. Astrophys.*, 2022, **663**, L2.

18 D. Loru, C. Cabezas, J. Cernicharo, M. Schnell and A. L. Steber, Detection of ethynylbenzene in TMC-1 and the interstellar search for 1,2-diethynylbenzene, *Astron. Astrophys.*, 2023, **677**, A166.

19 S. Thorwirth, P. Theule, C. A. Gottlieb, M. C. McCarthy and P. Thaddeus, Rotational Spectra of Small PAHs: Acenaphthene, Acenaphthylene, Azulene, and Fluorene, *Astrophys. J.*, 2007, **662**, 1309–1314.

20 A. D. Becke, A new mixing of Hartree–Fock and local density-functional theories, *J. Chem. Phys.*, 1993, **98**, 1372–1377.

21 T. H. Dunning, Gaussian basis sets for use in correlated molecular calculations. I. The atoms boron through neon and hydrogen, *J. Chem. Phys.*, 1989, **90**, 1007–1023.

22 M. J. Frisch, G. W. Trucks, H. B. Schlegel, G. E. Scuseria, M. A. Robb, J. R. Cheeseman, G. Scalmani, V. Barone, G. A. Petersson, H. Nakatsuji, X. Li, M. Caricato, A. V. Marenich, J. Bloino, B. G. Janesko, R. Gomperts, B. Mennucci, H. P. Hratchian, J. V. Ortiz, A. F. Izmaylov, J. L. Sonnenberg, D. Williams-Young, F. Ding, F. Lipparini, F. Egidi, J. Goings, B. Peng, A. Petrone, T. Henderson, D. Ranasinghe, V. G. Zakrzewski, J. Gao, N. Rega, G. Zheng, W. Liang, M. Hada, M. Ehara, K. Toyota, R. Fukuda, J. Hasegawa, M. Ishida, T. Nakajima, Y. Honda, O. Kitao, H. Nakai, T. Vreven, K. Throssell, J. A. Montgomery Jr., J. E. Peralta, F. Ogliaro, M. J. Bearpark, J. J. Heyd, E. N. Brothers, K. N. Kudin, V. N. Staroverov, T. A. Keith, R. Kobayashi, J. Normand, K. Raghavachari, A. P. Rendell, J. C. Burant, S. S. Iyengar, J. Tomasi, M. Cossi, J. M. Millam, M. Klene, C. Adamo, R. Cammi, J. W. Ochterski, R. L. Martin, K. Morokuma, O. Farkas, J. B. Foresman and D. J. Fox, *Gaussian 16, Revision C.01*, Gaussian, Inc., Wallin, 2016.

23 J. L. Neill, S. T. Shipman, L. Alvarez-Valtierra, A. Lesarri, Z. Kisiel and B. H. Pate, Rotational spectroscopy of iodobenzene and iodobenzene–neon with a direct digital 2–8 GHz chirped-pulse Fourier transform microwave spectrometer, *J. Mol. Spectrosc.*, 2011, **269**, 21–29.

24 C. Pérez, S. Lobsiger, N. A. Seifert, D. P. Zaleski, B. Temelso, G. C. Shields, Z. Kisiel and B. H. Pate, Broadband Fourier transform rotational spectroscopy for structure determination: The water heptamer, *Chem. Phys. Lett.*, 2013, **571**, 1–15.

25 C. Cabezas, J. Janeiro, D. Pérez, W. Li, M. Agúndez, A. L. Steber, E. Guitián, J. Demaison, C. Pérez, J. Cernicharo and A. Lesarri, Cyano-Polycyclic Aromatic Hydrocarbon Interstellar Candidates: Laboratory Identification, Equilibrium Structure and Astronomical Search of Cyanobiphenylene, *J. Phys. Chem. Lett.*, 2024, **15**, 7411–7418.

26 Z. Wang, X. Wang, Y. Ura and Y. Nishihara, Nickel-Catalyzed Decarbonylative Cyanation of Acyl Chlorides, *Org. Lett.*, 2019, **21**, 6779–6784.

27 C. Hsiao, Y. Lin, C. Liu, T. Wu and Y. Wu, Synthesis of Methylene-Bridge Polyarenes through Palladium-Catalyzed Activation of Benzylic Carbon-Hydrogen Bond, *Adv. Synth. Catal.*, 2010, **352**, 3267–3274.

28 X. Hou, Z. Ge, T. Wang, W. Guo, J. Wu, J. Cui, C. Lai and R. Li, Synthesis and Structure-Activity Relationships of A Novel Class of Dithiocarbamic Acid Esters as Anticancer Agent, *Arch. Pharm.*, 2011, **344**, 320–332.

29 H. M. Pickett, The fitting and prediction of vibration-rotation spectra with spin interactions, *J. Mol. Spectrosc.*, 1991, **148**, 371–377.

30 J. K. G. Watson, *Vibrational spectra and structure: A series of advances*, 1977, *vol. 6*, pp. 1–89.

31 W. Gordy and R. L. Cook, *Microwave molecular spectra*, Wiley, 1984.

32 M. Agúndez, N. Marcelino, B. Tercero and J. Cernicharo, Aromatic cycles are widespread in cold clouds, *Astron. Astrophys.*, 2023, **677**, L13.